



Effects of Spin Transition and Cation Substitution on the Optical Properties and Iron Partitioning in Carbonate Minerals

HU Jun^{1,2}, XU Liangxu², LIU Jin^{1,2,*} and YUE Donghui^{3,*}

¹ Center for High Pressure Science (CHiPS), State Key Laboratory of Metastable Materials Science and Technology, Yanshan University, Qinhuangdao, Hebei 066004, China

² Center for High Pressure Science and Technology Advanced Research, Beijing 100193, China

³ Heilongjiang Province Key Laboratory of Superhard Materials, Department of Physics, Mudanjiang Normal University, Mudanjiang, Heilongjiang 157012, China

Abstract: The high-pressure behavior of deep carbonate dictates the state and dynamics of oxidized carbon in the Earth's mantle, playing a vital role in the global carbon cycle and potentially influencing long-term climate change. Optical absorption and Raman spectroscopic measurements were carried out on two natural carbonate samples in diamond-anvil cells up to 60 GPa. Mg-substitution in high-spin siderite FeCO_3 increases the crystal field absorption band position by approximately 1000 cm^{-1} , but such an effect is marginal at $>40\text{ GPa}$ when entering the low-spin state. The crystal field absorption band of dolomite cannot be recognized upon compression to 45.8 GPa at room temperature but, in contrast, the high-pressure polymorph of dolomite exhibits a strong absorption band at frequencies higher than $(\text{Mg,Fe})\text{CO}_3$ in the low-spin state by $2000\text{--}2500\text{ cm}^{-1}$. Additionally, these carbonate minerals show more complicated features for the absorption edge, decreasing with pressure and undergoing a dramatic change through the spin crossover. The optical and vibrational properties of carbonate minerals are highly correlated with iron content and spin transition, indicating that iron is preferentially partitioned into low-spin carbonates. These results shed new light on how carbonate minerals evolve in the mantle, which is crucial to decode the deep carbon cycle.

Key words: carbonate petrology/mineralogy, mantle, high pressure, diamond-anvil cell, iron spin transition, iron partitioning, deep carbon cycle

Citation: Hu et al., 2023. Effects of Spin Transition and Cation Substitution on the Optical Properties and Iron Partitioning in Carbonate Minerals. Acta Geologica Sinica (English Edition), 97(1): 350–357. DOI: 10.1111/1755-6724.15042

1 Introduction

Subducting oceanic plates have been carrying down a substantial amount of carbonate into the Earth's mantle at subduction zones (Walter et al., 2011; Wang et al., 2018). Magnesite [MgCO_3], dolomite [$\text{CaMg}(\text{CO}_3)_2$] and their high-pressure polymorphs are the most promising deep-carbon carriers throughout the entire mantle, and their chemical and physical properties under high pressures are of the utmost importance to unraveling the carbon exchange between the shallow layers and deep interiors of the solid Earth (Sanchez-Valle et al., 2011; Hazen and Schiffries, 2013; Liu et al., 2014; Liu et al., 2016; Chao and Hsieh, 2019; Farsang et al., 2021). In particular, the evolution of these carbonate minerals in a subducted slab is crucial to constrain the global carbon cycle, and may impact long-term climate dynamics (Walker et al., 1981; Kerrick, 2001; Huybers and Langmuir, 2009; Kelemen et al., 2011; Malusà et al., 2018).

Thus far, the phase stability of subducted carbonate under deep-mantle conditions has been extensively investigated under both high-pressure and high-

temperature (P - T) conditions (Boulard et al., 2011; Lobanov et al., 2017; Dorfman et al., 2018; Sagatova et al., 2021). Magnesite and its high- P phases are reported as thermodynamically stable under the high P - T conditions of the deep mantle (Isshiki et al., 2004; Skorodumova et al., 2005; Oganov et al., 2008; Pickard and Needs, 2015; Marcondes et al., 2016; Santos et al., 2019; Binck et al., 2020a; Zhao et al., 2021). Notably, the phase boundaries and crystal structures of those high- P polymorphs remain contentious. Magnesite has a rhombohedral structure (space group $R\bar{3}c$) under ambient conditions, and it can undergo a structural transition into orthorhombic MgCO_3 -II phase at approximately 115 GPa (Isshiki et al., 2004). Recently, theoretical calculations have predicted that the high- P phase transition of MgCO_3 would occur at 75–85 GPa and the MgCO_3 -II phase might have different structures of $P\bar{1}$, $P2_1/c$, and $C2/m$ (Pickard and Needs, 2015; Li and Stackhouse, 2020). Comparatively, dolomite has a rhombohedral structure (space group $R\bar{3}$) with MgO_6 and CaO_6 units alternating along the c -axis on the Earth's surface, and its phase transitions are more complicated than magnesite under deep-mantle conditions. To date, a

* Corresponding author. E-mail: 15104409336@163.com; jinliuyc@foxmail.com

series of dolomite's high-*P* phases have been reported, including dolomite-II, -III, -IIIc, -IV, and -V (Mao et al., 2011; Merlini et al., 2012, 2017; Efthimiopoulos et al., 2017, 2018; Vennari and Williams, 2018; Binck et al., 2020b; Wang et al., 2022). Furthermore, magnesite, dolomite, and other carbonate minerals have frequently been discovered in superdeep diamond inclusions, evidencing that carbonate might exist in the mantle transition zone and the lower mantle (Kaminsky et al., 2009; Walter et al., 2011; Mazza et al., 2019).

Iron is ubiquitous in the mantle and core, based on the Earth's composition model (McDonough and Sun, 1995; Lü and Liu, 2022). It has been well perceived that FeCO₃ can be readily incorporated into the aforementioned carbonate minerals, forming a complete series of solid solutions especially with MgCO₃ (Lavina et al., 2009; Mao et al., 2011; Liu et al., 2015a). Thus far, the electronic spin-pairing transition of iron (IST) in carbonate minerals has been widely reported at mid-mantle pressures using theoretical calculations and high-*P* experiments with laser Raman spectroscopy and a battery of X-ray probes, including synchrotron Mössbauer spectroscopy, X-ray emission spectroscopy, X-ray absorption near edge structure, and X-ray diffraction (Mattila et al., 2007; Shi et al., 2008; Lavina et al., 2009; Lin et al., 2012; Spivak et al., 2014; Cerantola et al., 2015; Lobanov et al., 2016; Cerantola et al., 2019; Hsu et al., 2021). These previous studies have reached a consensus on the spin transition pressure and the width of the spin crossover of iron-bearing carbonate minerals. It should be noted that the IST is an isostructural transition without a space-group change for carbonate minerals. The high-spin to low-spin phase transition pressure range of iron-bearing magnesite [(Mg,Fe)CO₃] is very narrow within a few GPa of 45 GPa at room temperature, and high temperatures can moderately increase the onset pressure of the IST with a broadened spin crossover (Liu et al., 2014). Similarly, the high-*P* phase dolomite-III exhibits a drop of ~2% in the pressure-volume curve at ~47 GPa and room temperature, associated with the IST (Mao et al., 2011). The fact that the IST exerts significant influence on the chemical and physical properties of iron-bearing minerals in the deep mantle has been well established, as summarized in a recent review by Lin et al. (2013). For instance, iron-bearing carbonates have higher density, bulk modulus, and sound velocities in the low-spin state than in the high-spin state (Lin et al., 2012; Cerantola et al., 2015; Fu et al., 2017). Additionally, a thermal conductivity anomaly was reported in iron-rich magnesite [(Mg_{0.22}Fe_{0.78})CO₃] at 40–55 GPa and room temperature, highly related to the IST (Chao and Hsieh, 2019).

The IST not only influences physical properties, but also affects the crystal chemistry of mantle minerals (Lin et al., 2013). It can significantly alter the iron isotopic composition of mantle minerals (Liu et al., 2017; Yang et al., 2019). Moreover, the electronic spin-pairing transitions would change the partitioning behavior of iron among coexisting major lower-mantle minerals, ferropericlase [(Mg,Fe)O], bridgmanite [(Mg,Fe)SiO₃] and its high-*P* phase post-perovskite (Murakami et al., 2005). Similarly, there are a few studies looking into whether the

IST would lead to iron enrichment in carbonate minerals under mantle pressures using optical absorption measurements on a natural siderite sample [(Fe_{0.95}Mn_{0.05})CO₃] (Lobanov et al., 2015; Lobanov et al., 2016). On the basis of the derived crystal field stabilization energy (CFSE) of ferrous iron in siderite in the low-spin state, which is approximately one order of magnitude greater than that in the high-spin state, it has been proposed that the low-spin carbonate minerals would take in more ferrous iron from coexisting bridgmanite in the lower-mantle (Lobanov et al., 2015). To verify this hypothesis, it is indispensable to know how cation substitution (e.g., Mg²⁺) and varying iron concentrations affect the optical properties of iron-bearing carbonate minerals under Earth's mantle pressures.

In this study, we employ laser-heated diamond-anvil cell (DAC) techniques coupled with optical absorption and laser Raman spectroscopy, to investigate how the IST affects the optical properties of two natural carbonate samples with different iron contents from 1 bar to 60 GPa, iron-rich magnesite [(Mg_{0.38}Fe_{0.60}Mn_{0.02})CO₃], hereafter denoted as Sid60, and dolomite [(Mg_{0.38}Fe_{0.10}Mn_{0.01}Ca_{0.51})CO₃], hereafter denoted as Dol10.

2 Materials and Methodology

Two natural iron-bearing carbonate single-crystal samples were explored in this study.

2.1 Sid60

An iron-bearing magnesite Sid60 sample was obtained from the American Museum of Natural History (AMNH No. NMNH 40298); its thermoelastic properties have previously been experimentally investigated up to 8.9 GPa by Zhang et al. (1998). X-ray diffraction and electron microprobe analyses (EPMA) confirmed that it has rhombohedral structure (space group *R* $\bar{3}c$) with lattice parameters *a* = 4.6719 (5) Å and *c* = 15.2517(53) Å under ambient conditions and exhibits a homogeneous chemical composition, (Mg_{0.38}Fe_{0.60}Mn_{0.02})CO₃ with minor CaCO₃ less than 1 mol%.

2.2 Dol10

An iron-bearing dolomite Dol10 sample which was collected from Shangpu mining area (Hunan Province, China) has a chemical composition of (Mg_{0.38}Fe_{0.10}Mn_{0.01}Ca_{0.51})CO₃. Its phase stability and vibrational properties have previously been studied up to 58 GPa by Zhao et al. (2020).

2.3 Methods

Cleaved single-crystal samples were hand-picked under an optical microscope and then loaded into symmetric DACs with culets of 300 μm in diameter.

The loaded samples were 60–70 μm in diameter and 8–10 μm thick with the use of neon as a pressure-transmitting medium. Rhenium gaskets were indented to ~30 μm thick, and a hole of 150–160 μm in diameter was then laser-drilled at the center of the indentation serving as a sample chamber. Two ruby spheres were placed next to the sample and the pressure was averaged over the

multiple measurements of ruby fluorescence before and after spectrum collection (Mao et al., 1986).

High- P Raman and optical absorption spectra were recorded using the Raman system in the DEEP Laboratory and the UV-NIR absorption spectroscopy at the Center for High Pressure Science and Technology Advanced Research (HPSTAR), Beijing. The Raman system was calibrated by the Raman signal of a Si wafer, equipped with a Coherent Verdi V2 laser of 532 nm wavelength and PIXIS 400 imaging spectrometer coupled with 1800 lines/mm ruled grating. The laser power was at 20–50 mW to reduce heat on the sample, and each Raman spectrum was taken in the range of 100–1300 cm^{-1} with an exposure time of ~ 5 mins.

Optical absorption measurements were recorded using a Xeon light source between 400 and 1000 nm. The absorption spectra were obtained in a homemade spectroscopy system in the microregion (Gora-UVN-FL) by Shanghai Ideaoptics Corp., Ltd. All absorption spectra were collected at room temperature and absorption bands were fitted to the Voigt functions with an uncertainty of ~ 1000 cm^{-1} . Additionally, the absorption edge was evaluated by extrapolating the linear portion of the absorption coefficient versus wavenumber.

3 Results

3.1 Iron-rich magnesite—Sid60 and Sid95

We carried out Raman and absorption spectroscopic measurements on Sid60 in 2–5 GPa intervals up to 57.3 GPa at room temperature. Fig. 1 shows representative Raman spectra of Sid60 as a function of pressure. At ambient conditions, four Raman active modes were

observed at 191.8, 299.4, 735.4, and 1088.8 cm^{-1} , corresponding to the translational (T) and librational (L) lattice modes and in-plane bend (ν_4) and symmetric stretch (ν_1) internal modes, respectively (Fig. 1). These modes are consistent with FeCO_3 (AMNH no. NMNH R11313) and $(\text{Mg}_{0.33}\text{Fe}_{0.65}\text{Mn}_{0.02})\text{CO}_3$ (denoted as Sid65, no. V3817 from the Vargas Gem and Mineral Collection at the University of Texas at Austin) (Lin et al., 2012; Zhao et al., 2020). The observed moderate changes in Raman shifts reflect the Mg-substitution effects on the lattice vibrations of carbonate minerals at ambient conditions.

The IST pressure in Sid60 is approximately at 41.5 GPa, evidenced by a dramatic reduction of ~ 30 cm^{-1} in the symmetric stretch (ν_1) Raman band from 36.1 to 41.5 GPa. Across the IST, these iron-bearing magnesites undergo unit-cell volume collapses by several percentages, highly related to iron content (Lavina et al., 2009, 2010a, 2010b; Lin et al., 2012; Liu et al., 2014; Liu et al., 2015b). Such large volume collapses lengthen the C–O bonding in the rigid CO_3^{2-} unit from high-spin to low-spin states, resulting in the aforementioned decrease in the Raman shift of the ν_1 mode (Lavina et al., 2010b; Lin et al., 2012).

Interestingly, the color of the Sid60 sample is optically transparent in the high-spin state, but changes to partially green at 41.5–46.5 GPa, where the high-spin and low-spin states coexist at room temperature. Note that such color changes have been consistently reported in the MgCO_3 – FeCO_3 solid solutions at 40–50 GPa (Lavina et al., 2009; Liu et al., 2014; Lobanov et al., 2015; Zhao et al., 2020). This indicates that the IST pressure of our Sid60 sample is in good agreement with previous studies. The color evolution as a function of pressure vividly demonstrates the dramatic changes in the optical properties of the Sid60

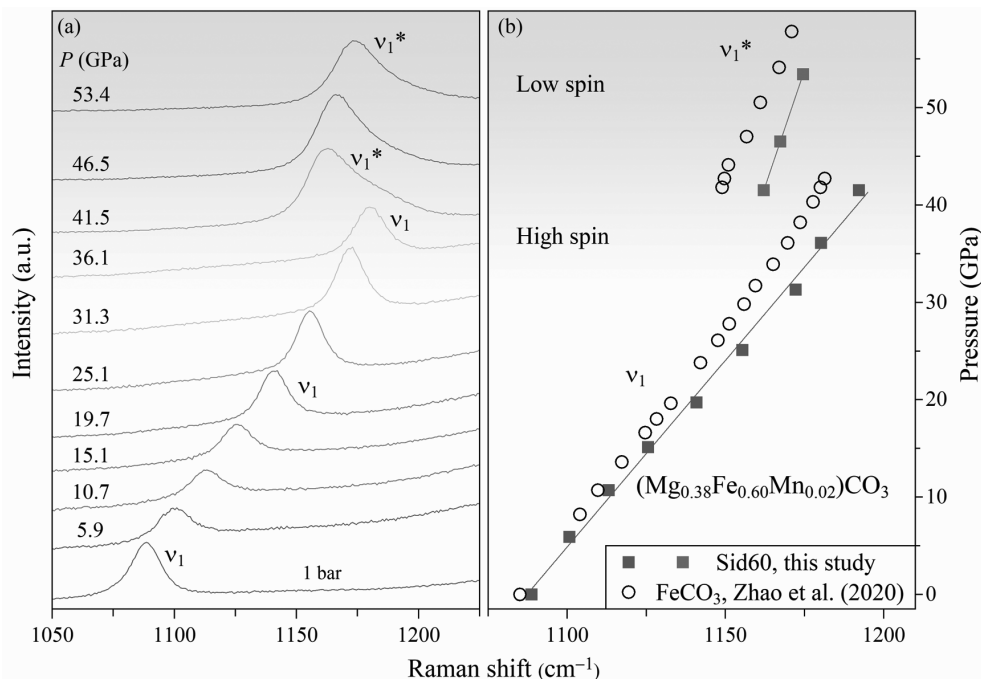


Fig. 1. Representative Raman spectra of Sid60 (a) and the pressure evolution of Raman shift (b) throughout the electronic spin-pairing transition of iron (this study compared with Zhao et al. 2020).

Red and blue squares represent the high- and low-spin states, respectively.

sample. Across the IST, iron's *d*-orbital electrons rearrange upon the increased energy separation between the ground and excited electronic states (Burns, 1993). Such dramatic changes can significantly influence the local structure of FeO₆ octahedra, leading to the visible color changes of the Sid60 sample under high pressures. Fig. 2 shows the optical absorption spectra of the Sid60 sample collected with increasing pressure from 1 bar to 57.3 GPa at room temperature. No absorption band is present at 11000–25000 cm⁻¹ for Sid60 under ambient conditions, while a weak and broad absorption band was observed at 10325 cm⁻¹ for Fe_{0.95}Mn_{0.05}CO₃, hereafter denoted as Sid95, by Lobanov et al. (2015). This band reflects the CFSE of Fe²⁺ in an octahedral field, corresponding to the electronic transition from ⁵T_{2g} to ⁵E_g states in high-spin (Mg,Fe)CO₃, which is the only spin-allowed transition of the ⁵T_{2g} ground state. As pressure increases, a relatively weak and broad absorption band centered at approximate 12500 cm⁻¹ emerges at 19.7 GPa for high-spin Sid60, and it remains pretty weak in the high-spin state and blueshifts to 14350 cm⁻¹ at 36.1 GPa, with a pressure dependence of 103 ± 7 cm⁻¹/GPa (Fig. 3). Similarly, the absorption band

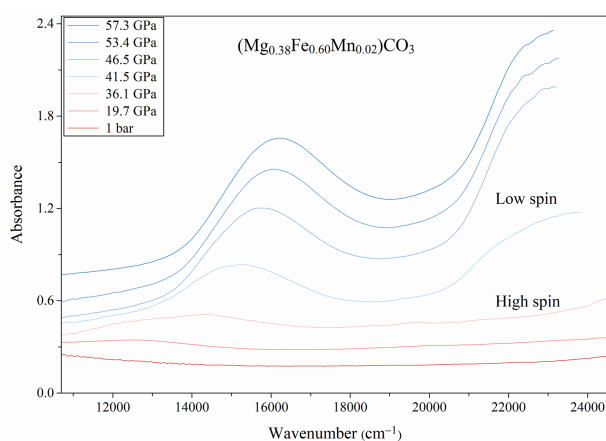


Fig. 2. Representative optical absorption spectra of Sid60 under high pressures.

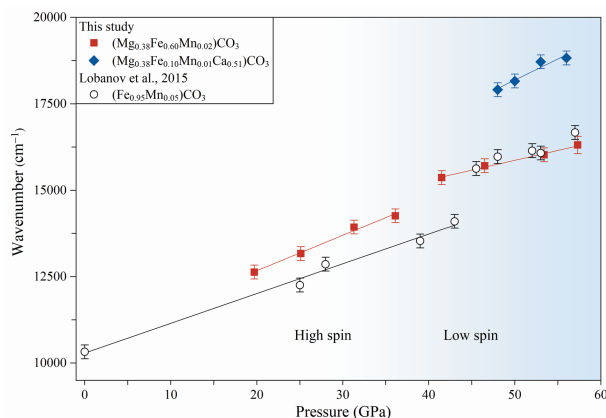


Fig. 3. The center position of absorption bands of iron-bearing carbonate minerals under high pressures (this study compared with Lobanov et al. 2015).

The shaded area represents carbonates in the low-spin state. The solid lines are the linear fit to experimental data.

of high-spin Sid95 increases monotonically from 12256 cm⁻¹ at 25 GPa to 13532 cm⁻¹ at 39 GPa with a pressure dependence of 88 ± 5 cm⁻¹/GPa (Lobanov et al., 2015). Therefore, the splitting energy between ⁵T_{2g} and ⁵E_g orbitals increases as pressure rises, resulting in the blueshift of the crystal field band.

Mg-substitution has distinct effects on the absorption band position as well as its pressure dependence between high-spin and low-spin (Mg,Fe)CO₃ under high pressures. As we can see, the pressure dependence of the absorption band is increased by about 15% from Sid95 to Sid60, while the absorption band position is elevated by ~650 cm⁻¹ at 19.7 GPa and ~900 cm⁻¹ at 36.1 GPa in the high-spin state (Fig. 3). This result indicates that 35 mol% Mg-substitution can moderately blueshift the absorption band and increase the pressure dependence from high-spin Sid95 to Sid60. The shape of the absorption band of high-spin Sid95 is symmetrical with only one maximum value, indicating that FeO₆ octahedra are not distorted (Lavina et al., 2009). Notably, the shape of the absorption band of Sid95 becomes less symmetrical in the low-spin state, mainly because the IST can cause the distortion of FeO₆

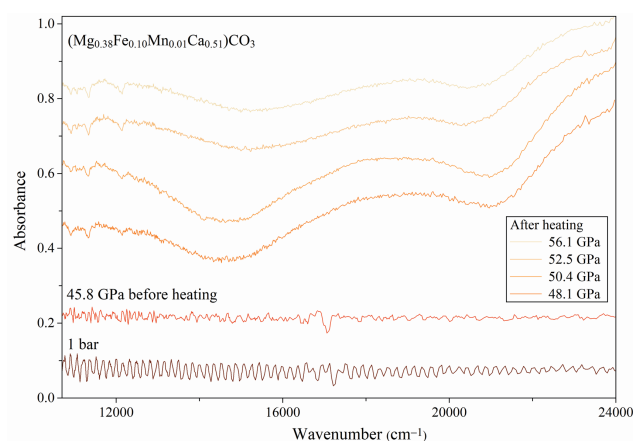


Fig. 4. Representative optical absorption spectra of Dol10 under high pressures.

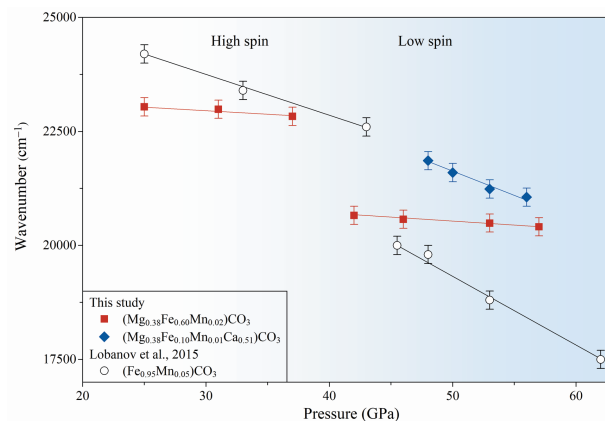


Fig. 5. The position of the absorption edge of carbonate minerals with increasing pressure (this study compared with Lobanov et al., 2015).

The shaded area represents carbonate minerals in the low-spin state. The solid lines are the linear fit to experimental data.

octahedra to some extent (Lavina et al., 2009; Lobanov et al., 2015). Similarly, the shape of the absorption band of high-spin Sid60 is less symmetrical with respect to high-spin Sid95, suggesting that the high degree of Mg-substitution could also make the FeO_6 octahedra slightly distorted in Sid60. However, these effects become negligible between the Sid95 and Sid60 samples in the low-spin state. The main absorption band corresponds to the electronic transition from ${}^1A_{1g}$ to ${}^1T_{1g}$ in the low-spin Sid60 and Sid95 samples, which exhibits the lowest energy among all spin-allowed transitions (Lobanov et al., 2015).

The low-spin state has a greater absorption magnitude than the high-spin state for the $(\text{Mg,Fe})\text{CO}_3$ solid solutions under high pressures (Figs. 2–3). This effect is mainly due to the minimal changes in overall optical absorption of $(\text{Mg,Fe})\text{CO}_3$ in the high-spin state. By contrast, an evident rise in absorption emerges at frequencies higher than 20500 cm^{-1} for the low-spin Sid65 at 41.5 GPa. A comparable rise was also observed in Sid95 at 39 GPa and this band has been assigned to Fe-O electron transfer in FeO_6 octahedra. The metal-oxygen charge transfer transitions generally feature the comparable position and intensity of this absorption edge, which tends to redshift with increasing pressure (Lobanov et al., 2015). Further, the absorption band of low-spin Sid60 increases approximately from 15368 cm^{-1} at 41.5 GPa to 16310 cm^{-1} at 57.3 GPa, with a pressure dependence of $57 \pm 4\text{ cm}^{-1}/\text{GPa}$. Note that the absorption band of low-spin Sid60 is comparable to that of low-spin Sid95 at a given pressure up to 60 GPa. This is likely ascribed to the FeO_6 octahedra being distorted to the same degree for Sid60 and Sid95 when entering the low-spin state (Lavina et al., 2009).

3.2 Dolomite (Dol10)

In order to investigate how Ca-substitution affects the optical properties of mantle carbonate minerals under high pressures, we also conducted absorption spectroscopic measurements on the Dol10 sample in ~ 5 GPa intervals up to 60 GPa. Intriguingly, there were no absorption bands recognized in the spectra of the Dol10 sample collected under high pressures and room temperature before it was laser heated (Fig. 4). We note that the Raman spectra of Dol10 were collected as a function of pressure, indicating the sample undergoes a series of phase transitions from dolomite-I to dolomite-Ib approximately at 8 GPa, and then to dolomite-II at 15 GPa and dolomite-IIIb phase at 36 GPa, as illustrated in Zhao et al. (2020). Meanwhile, there are no visible color changes or dramatic reductions in the symmetrical stretch (ν_1) Raman band in the Dol10 sample up to 60 GPa, because no IST occurs in this sample upon cold compression at room temperature. These results suggest Ca-substitution exhibits greater effects on the IST and optical properties of mantle carbonate minerals than Mg-substitution, probably because the effective ionic radii of Mg^{2+} are closer to that of Fe^{2+} in the octahedral coordination geometry.

Subsequently, the Dol10 sample was laser heated to 1500–1600 K at 60 GPa but the pressure was decreased to 56.1 GPa after heating. The sample transformed into a

new monoclinic phase (dolomite-III), which was observed between 36 and 83 GPa by Mao et al. (2011). We collected the absorption spectra of the laser-heated Dol10 sample with decreasing pressure down to ambient pressure (Fig. 4). The absorption spectra taken from 56.1 to 48.1 GPa feature a moderate to strong absorption band centered at $\sim 18000\text{ cm}^{-1}$; this could originate from the temperature-induced asymmetrical broadening and redshift of the absorption band from ${}^1A_{1g}$ to ${}^1T_{1g}$ orbitals. However, the absorption spectra became relatively flat again and the absorption band was no longer visible when the pressure was decreased below 40–45 GPa. This might be related to the amorphization of the quenched sample upon decompression, or it might also be associated with the IST occurring in the dolomite-III phase of Dol10. This was reported at ~ 47 GPa with the evidence of a dramatic change of $\sim 2\%$ in the unit cell volume for the dolomite-III phase by Mao et al. (2011). In other words, no absorption band or one extremely weak band exists in the high-spin dolomite-III phase, whereas there is an absorption band visible in the optical absorption spectra of the low-spin dolomite-III phase. Moreover, the color of the sample changed dramatically from optically transparent to black and opaque, which is consistent with the measured position of the absorption edge (Fig. 5). The positions of the absorption edge were determined following the same method of Lobanov et al. (2015) by fitting the optical absorption spectra with the energy dependence characteristics for a direct band gap. Notably, Fig. 5 shows that the high-spin state has relatively greater values than the low-spin state for the position of the absorption edge of carbonate minerals. Such a large pressure-induced redshift of the absorption edge was observed for Sid95 and Sid60 from the high-spin to low-spin state, reaching ~ 2600 and $\sim 1850\text{ cm}^{-1}$, respectively. Moreover, the position values of the absorption edge of the low-spin dolomite-III phase of Dol10 are overall greater than that of low-spin Sid60 and Sid95 between 45 and 60 GPa, likely associated with the iron concentrations in carbonate minerals.

4 Discussion

Carbonated slabs could have penetrated the boundary between the mantle transition zone and the uppermost lower mantle, even reaching the base of the lower mantle (Zhang et al., 2022). During subduction, iron-bearing carbonate minerals not only undergo a pressure-induced spin-pairing transition, but also exchange cations like Fe^{2+} , Mg^{2+} , and Ca^{2+} with surrounding mantle minerals. Lobanov et al. (2015) demonstrated that these optical properties and the IST are highly related to the crystal chemistry of iron-bearing carbonate minerals. In particular, the derived CFSE values from the absorption band contribute to the enthalpy terms of the Gibbs free energy, which can greatly influence the partitioning coefficient (K) (Lobanov et al., 2015). They also pointed out that iron-bearing carbonate Sid95 in the low-spin state shows strongly negative values of $\ln K$ with respect to bridgmanite that is the most abundant mineral in the lower mantle. For instance, it reaches -29 at 45 GPa and 2500

K, indicating that the lower-mantle carbonate minerals would become iron-enriched and even close to pure FeCO_3 in equilibrium with bridgmanite $[(\text{Mg,Fe})\text{SiO}_3]$. The Sid95 and Sid60 samples in the low-spin state almost have the same center position values of the absorption bands, suggesting that this tendency could be applied to the entire solid solutions of $(\text{Fe,Mg})\text{CO}_3$ in the low-spin state under mid-mantle pressures.

Remarkably, the low-spin dolomite-III phase of Dol10 exhibits the maximum absorption band among the three carbonate minerals at ~ 50 GPa, as illustrated in Fig. 3. The difference can be as large as 2500 cm^{-1} . Hence, it is expected that the incorporation of Ca into $(\text{Fe,Mg})\text{CO}_3$ would cause iron redistribution among these carbonate minerals across the spin transition at mid-mantle depths. Moreover, the IST width can be significantly broadened by elevated temperatures for mantle carbonate, as pointed out by Liu et al. (2014). In particular, the major lower-mantle minerals, e.g., ferroperricite and bridgmanite, have higher IST pressures with much more broader widths (Lin et al., 2013). This suggests that iron redistribution processes might occur throughout the mid-mantle and even to the core–mantle boundary region. We note that such a chemical redistribution is expected to influence the deep carbon cycle significantly, especially through the thermodynamic stability of carbonate in the lower mantle. Recent studies reported that iron-enriched carbonate minerals with planar CO_3^{2-} units would undergo a phase transition to form CO_4^{4-} tetrahedra under deep lower-mantle conditions, accompanied by complex self-redox reactions to produce elemental carbon (Boulard et al., 2012; Cerantola et al., 2017). When coexisting with major lower-mantle minerals and entering the low-spin state, these carbonate minerals could exhibit higher iron concentrations with increasing depths, likely resulting in carbonate reduction to form diamond and iron carbides (Dorfman et al., 2018; Drewitt et al., 2019). Therefore, the IST and compositional variations, as well as the consequent distinct optical properties could have affected the fate of carbonate minerals in the mantle and the deep carbon cycle through iron partitioning among the mantle phases.

5 Conclusions

In this study, we collected the optical absorption and laser Raman spectra on samples Sid60 $[(\text{Mg}_{0.38}\text{Fe}_{0.60}\text{Mn}_{0.02})\text{CO}_3]$ and Dol10 $[(\text{Mg}_{0.38}\text{Fe}_{0.10}\text{Mn}_{0.01}\text{Ca}_{0.51})\text{CO}_3]$ up to 60 GPa at room temperature. We found that the Mg-substitution has distinct influences on the crystal field absorption band of siderite $[\text{FeCO}_3]$ between the high-spin and low-spin states. It is also evident that the high- P phase of dolomite in the low-spin state exhibits a strong absorption band at frequencies higher than the FeCO_3 – MgCO_3 system. Furthermore, the pressure dependence of the absorption edge is very different between siderite and the two carbonate samples investigated in this study.

Our results suggest that the effects of compositional variations and the iron spin transition (IST) on the optical properties and iron partitioning of carbonate minerals should not be neglected, providing new constraints on the

role of mantle carbonates in the deep carbon cycle. The IST significantly affects the optical properties of the two studied natural carbonate samples under high pressures. Moreover, varying cation concentrations of Mg^{2+} , Fe^{2+} , and Ca^{2+} can exert distinct effects on the crystal field absorption band of mantle carbonate minerals.

The above factors might dictate how iron and other metal elements (e.g., Ca, Mg, and Zn) exchange between carbonate and coexisting mantle minerals. Such an exchange might have contributed to iron, zinc, calcium, and magnesium isotopic signatures observed in basalts (Li et al., 2017; Liu et al., 2017; Zhang et al., 2022), and this demands further work.

Acknowledgments

This work is supported by the National Key Research and Development Program of China (Grant No. 2019YFA0708502). Some experiments were supported by the Synergic Extreme Condition User Facility (SECUF). We thank Ma Yingying, Zhao Chaoshuai, Wang Lijuan, Li Kuo, and Wang Yonggang for their experimental assistance and constructive discussion.

Manuscript received Oct. 29, 2022

accepted Jan. 17, 2023

associate EIC: ZHANG Lifei

edited by Susan TURNER and GUO Xianqing

References

- Binck, J., Bayarjargal, L., Lobanov, S.S., Morgenroth, W., Luchitskaia, R., Pickard, C.J., Milman, V., Refson, K., Jochym, D.B., Byrne, P., and Winkler, B., 2020a. Phase stabilities of MgCO_3 and MgCO_3 -II studied by Raman spectroscopy, X-ray diffraction, and density functional theory calculations. *Physical Review Letters*, 4: 055001.
- Binck, J., Chariton, S., Stekiel, M., Bayarjargal, L., Morgenroth, W., Milman, V., Dubrovinsky, L., and Winkler, B., 2020b. High-pressure, high-temperature phase stability of iron-poor dolomite and the structures of dolomite-IIIc and dolomite-V. *Physics of the Earth and Planetary Interiors*, 299: 106403.
- Boulard, E., Gloter, A., Corgne, A., Antonangeli, D., Auzende, A.L., Perrillat, J.P., Guyot, F., and Fiquet, G., 2011. New host for carbon in the deep Earth. *Proceedings of the National Academy of Sciences of the United States of America*, 108: 5184–5187.
- Boulard, E., Menguy, N., Auzende, A.L., Benzerara, K., Bureau, H., Antonangeli, D., Corgne, A., Morard, G., Siebert, J., Perrillat, J.P., Guyot, F., and Fiquet, G., 2012. Experimental investigation of the stability of Fe-rich carbonates in the lower mantle. *Journal of Geophysical Research*, 117: B02208.
- Burns, R.G., 1993. *Mineralogical Applications of Crystal Field Theory*. Cambridge, UK: Cambridge University Press.
- Cerantola, V., Bykova, E., Kuppenko, I., Merlini, M., Ismailova, L., McCammon, C., Bykov, M., Chumakov, A.I., Petitgirard, S., Kantor, I., Svitlyk, V., Jacobs, J., Hanfland, M., Mezouar, M., Prescher, C., Ruffer, R., Prakapenka, V.B., and Dubrovinsky, L., 2017. Stability of iron-bearing carbonates in the deep Earth's interior. *Nature Communications*, 8: 15960.
- Cerantola, V., McCammon, C., Kuppenko, I., Kantor, I., Marini, C., Wilke, M., Ismailova, L., Solopova, N., Chumakov, A., Pascarelli, S., and Dubrovinsky, L., 2015. High-pressure spectroscopic study of siderite (FeCO_3) with a focus on spin crossover. *American Mineralogist*, 100: 2670–2681.
- Cerantola, V., Wilke, M., Kantor, I., Ismailova, L., Kuppenko, I., McCammon, C., Pascarelli, S., and Dubrovinsky, L.S., 2019. Experimental investigation of FeCO_3 (siderite) stability in Earth's lower mantle using XANES spectroscopy. *American*

- Mineralogist, 104: 1083–1091.
- Chao, K.H., and Hsieh, W.P., 2019. Thermal conductivity anomaly in $(\text{FeO}_{.78}\text{MgO}_{.22})\text{CO}_3$ siderite across spin transition of iron. *Journal of Geophysical Research*, 124: 1388–1396.
- Dorfman, S.M., Badro, J., Nabiei, F., Prakapenka, V.B., Cantoni, M., and Gillet, P., 2018. Carbonate stability in the reduced lower mantle. *Earth and Planetary Science Letters*, 489: 84–91.
- Drewitt, J.W.E., Walter, M.J., Zhang, H., McMahon, S.C., Edwards, D., Heinen, B.J., Lord, O.T., Anzellini, S., and Klepepe, A.K., 2019. The fate of carbonate in oceanic crust subducted into Earth's lower mantle. *Earth and Planetary Science Letters*, 511: 213–222.
- Efthimiopoulos, I., Germer, M., Jahn, S., Harms, M., Reichmann, H.J., Speziale, S., Schade, U., Sieber, M., and Koch-Müller, M., 2018. Effects of hydrostaticity on the structural stability of carbonates at lower mantle pressures: The case study of dolomite. *High Pressure Research*, 1–14.
- Efthimiopoulos, I., Jahn, S., Kuras, A., Schade, U., and Koch-Müller, M., 2017. Combined high-pressure and high-temperature vibrational studies of dolomite: Phase diagram and evidence of a new distorted modification. *Physics and Chemistry of Minerals*, 44: 465–476.
- Farsang, S., Louvel, M., Zhao, C., Mezouar, M., Rosa, A.D., Widmer, R.N., Feng, X., Liu, J., and Redfern, S.A.T., 2021. Deep carbon cycle constrained by carbonate solubility. *Nature Communications*, 2: 1–9.
- Fu, S., Yang, J., and Lin, J.F., 2017. Abnormal elasticity of single-crystal magnesiosiderite across the spin transition in Earth's lower mantle. *Physical Review Letters*, 118: 036402.
- Hazen, R.M., and Schiffrins, C.M., 2013. Why deep carbon? *Reviews in Mineralogy and Geochemistry*, 75: 1–6.
- Hsu, H., Crisostomo, C.P., Wang, W., and Wu, Z., 2021. Anomalous thermal properties and spin crossover of ferromagnesite $(\text{Mg,Fe})\text{CO}_3$. *Physical Review B*, 103: 054401.
- Huybers, P., and Langmuir, C., 2009. Feedback between deglaciation, volcanism, and atmospheric CO_2 . *Earth and Planetary Science Letters*, 286: 479–491.
- Isshiki, M., Irifune, T., Hirose, K., Ono, S., Ohishi, Y., Watanuki, T., Nishibori, E., Takata, M., and Sakata, M., 2004. Stability of magnesite and its high-pressure form in the lowermost mantle. *Nature*, 427: 60–63.
- Kaminsky, F., Wirth, R., Matsyuk, S., Schreiber, A., and Thomas, R., 2009. Nyerereite and nahcolite inclusions in diamond: Evidence for lower-mantle carbonatitic magmas. *Mineralogical Magazine*, 73: 797–816.
- Kelemen, P., Matter, J., Falk, E., Rudge, J., Curry, W., and Blusztajn, J., 2011. Rates and mechanisms of mineral carbonation in peridotite: Natural processes and recipes for enhanced, in situ CO_2 capture and storage. *Annual Review of Earth and Planetary Sciences*, 39: 545–576.
- Kerrick, D.M., 2001. Present and past nonanthropogenic CO_2 degassing from the solid Earth. *Reviews of Geophysics*, 39: 565–585.
- Lavina, B., Dera, P., Downs, R.T., Prakapenka, V., Rivers, M., Sutton, S., and Nicol, M., 2009. Siderite at lower mantle conditions and the effects of the pressure-induced spin-pairing transition. *Geophysical Research Letters*, 36: L23306.
- Lavina, B., Dera, P., Downs, R.T., Tschauer, O., Yang, W., Shebanova, O., and Shen, G., 2010a. Effect of dilution on the spin pairing transition in rhombohedral carbonates. *Geophysical Research Letters*, 30: 224–229.
- Lavina, B., Dera, P., Downs, R.T., Yang, W., Sinogeikin, S., Meng, Y., Shen, G., and Schiffrin, D., 2010b. Structure of siderite FeCO_3 to 56 GPa and hysteresis of its spin-pairing transition. *Physical Review B*, 82: 064110.
- Li, S.G., Yang, W., Ke, S., Meng, X., Tian, H., Xu, L., He, Y., Huang, J., Wang, X.C., Xia, Q., Sun, W., Yang, X., Ren, Z.Y., Wei, H., Liu, Y.S., Meng, F., and Yan, J., 2017. Deep carbon cycles constrained by a large-scale mantle Mg isotope anomaly in eastern China. *National Science Review*, 4: 111–120.
- Li, Z., and Stackhouse, S., 2020. Iron-rich carbonates stabilized by magnetic entropy at lower mantle conditions. *Earth and Planetary Science Letters*, 531: 115959.
- Lin, J.F., Liu, J., Jacobs, C., and Prakapenka, V.B., 2012. Vibrational and elastic properties of ferromagnesite across the electronic spin-pairing transition of iron. *American Mineralogist*, 97: 583–591.
- Lin, J.F., Speziale, S., Mao, Z., and Marquardt, H., 2013. Effects of the electronic spin transitions of iron in lower mantle minerals: Implications for deep mantle geophysics and geochemistry. *Reviews of Geophysics*, 51: 244–275.
- Liu, J., Caracas, R., Fan, D., Bobocioiu, E., Zhang, D., and Mao, W.L., 2016. High-pressure compressibility and vibrational properties of $(\text{Ca,Mn})\text{CO}_3$. *American Mineralogist*, 101: 2723–2730.
- Liu, J., Dauphas, N., Roskosz, M., Hu, M.Y., Yang, H., Bi, W., Zhao, J., Alp, E.E., Hu, J.Y., and Lin, J.F., 2017. Iron isotopic fractionation between silicate mantle and metallic core at high pressure. *Nature Communications*, 8: 14377.
- Liu, J., Lin, J.F., Mao, Z., and Prakapenka, V.B., 2014. Thermal equation of state and spin transition of magnesiosiderite at high pressure and temperature. *American Mineralogist*, 99: 84–93.
- Liu, J., Lin, J.F., and Prakapenka, V.B., 2015a. High-pressure orthorhombic ferromagnesite as a potential deep-mantle carbon carrier. *Scientific Reports*, 5: 7640.
- Liu, Z., Irifune, T., Gréaux, S., Arimoto, T., Shinmei, T., and Higo, Y., 2015b. Elastic wave velocity of polycrystalline $\text{Mg}_80\text{Py}_{20}$ garnet to 21 GPa and 2,000 K. *Physics and Chemistry of Minerals*, 42: 213–222.
- Lobanov, S.S., Dong, X., Martirosyan, N.S., Samtsevich, A.I., Stevanovic, V., Gavryushkin, P.N., Litasov, K.D., Greenberg, E., Prakapenka, V.B., Oganov, A.R., and Goncharov, A.F., 2017. Raman spectroscopy and X-ray diffraction of sp^3 CaCO_3 at lower mantle pressures. *Physical Review B*, 96: 104101.
- Lobanov, S.S., Goncharov, A.F., and Litasov, K.D., 2015. Optical properties of siderite (FeCO_3) across the spin transition: Crossover to iron-rich carbonates in the lower mantle. *American Mineralogist*, 100: 1059–1064.
- Lobanov, S.S., Holtgrewe, N., and Goncharov, A.F., 2016. Reduced radiative conductivity of low spin FeO_6 -octahedra in FeCO_3 at high pressure and temperature. *Earth and Planetary Science Letters*, 449: 20–25.
- Lü, C., and Liu, J., 2022. Early planetary processes and light elements in iron-dominated cores. *Acta Geochimica*, 41: 625–649.
- Malusà, M., Frezzotti, M.L., Ferrando, S., Brandmayr, E., Romanelli, F., and Panza, G., 2018. Active carbon sequestration in the Alpine mantle wedge and implications for long-term climate trends. *Scientific Reports*, 8: 4740.
- Mao, H.K., Xu, J., and Bell, P.M., 1986. Calibration of the Ruby pressure gauge to 800 kbar under quasi-hydrostatic conditions. *Journal of Geophysical Research*, 91: 4673–4676.
- Mao, Z., Armentrout, M., Rainey, E., Manning, C.E., Dera, P., Prakapenka, V.B., and Kavner, A., 2011. Dolomite III: A new candidate lower mantle carbonate. *Geophysical Research Letters*, 38: L22303.
- Marcondes, M.L., Justo, J.F., and Assali, L.V.C., 2016. Carbonates at high pressures: Possible carriers for deep carbon reservoirs in the Earth's lower mantle. *Physical Review B*, 94: 104112.
- Mattila, A., Pykkänen, T., Rueff, J.P., Huotari, S., Vankó, G., Hanfland, M., Lehtinen, M., and Hämäläinen, K., 2007. Pressure induced magnetic transition in siderite FeCO_3 studied by X-ray emission spectroscopy. *Journal of Physics Condensed Matter*, 19: 386206.
- Mazza, S.E., Gazel, E., Bizimis, M., Moucha, R., Béguélin, P., Johnson, E.A., McAleer, R.J., and Sobolev, A.V., 2019. Sampling the volatile-rich transition zone beneath Bermuda. *Nature*, 569: 398–403.
- McDonough, W.F., and Sun, S.S., 1995. The composition of the Earth. *Chemical Geology*, 120: 223–253.
- Merlini, M., Cerantola, V., Gatta, G.D., Gemmi, M., Hanfland, M., Kuppenko, I., Lotti, P., Müller, H., and Zhang, L., 2017. Dolomite-IV: Candidate structure for a carbonate in the Earth's lower mantle. *American Mineralogist*, 102: 1763–

- 1766.
- Merlini, M., Crichton, W.A., Hanfland, M., Gemmi, M., Müller, H., Kuppenko, I., and Dubrovinsky, L., 2012. Structures of dolomite at ultrahigh pressure and their influence on the deep carbon cycle. *Proceedings of the National Academy of Sciences of the United States of America*, 109: 13509–13514.
- Murakami, M., Hirose, K., Sata, N., and Ohishi, Y., 2005. Postperovskite phase transition and mineral chemistry in the pyrolytic lowermost mantle. *Geophysical Research Letters*, 32: L03304.
- Oganov, A.R., Ono, S., Ma, Y., Glass, C.W., and Garcia, A., 2008. Novel high-pressure structures of MgCO₃, CaCO₃ and CO₂ and their role in Earth's lower mantle. *Earth and Planetary Science Letters*, 273: 38–47.
- Pickard, C.J., and Needs, R.J., 2015. Structures and stability of calcium and magnesium carbonates at mantle pressures. *Physical Review B*, 91: 7.
- Sagatova, D.N., Shatskiy, A.F., Gavryushkin, P.N., Sagatov, N.E., and Litasov, K.D., 2021. Stability of Ca₂CO₄-*Pnma* against the main mantle minerals from ab initio computations. *ACS Earth and Space Chemistry*, 5: 1709–1715.
- Sanchez-Valle, C., Ghosh, S., and Rosa, A.D., 2011. Sound velocities of ferromagnesian carbonates and the seismic detection of carbonates in eclogites and the mantle. *Geophysical Research Letters*, 38: L24315.
- Santos, S.S.M., Marcondes, M.L., Justo, J.F., and Assali, L.V.C., 2019. Stability of calcium and magnesium carbonates at Earth's lower mantle thermodynamic conditions. *Earth and Planetary Science Letters*, 506: 1–7.
- Shi, H., Luo, W., Johansson, B., and Ahuja, R., 2008. First-principles calculations of the electronic structure and pressure-induced magnetic transition in siderite FeCO₃. *Physical Review B*, 78: 155119.
- Skorodumova, N.V., Belonoshko, A.B., Huang, L., Ahuja, R., and Johansson, B., 2005. Stability of the MgCO₃ structures under lower mantle conditions. *American Mineralogist*, 90: 1008–1011.
- Spivak, A., Solopova, N., Cerantola, V., Bykova, E., Zakharchenko, E., Dubrovinsky, L., and Litvin, Y., 2014. Raman study of MgCO₃-FeCO₃ carbonate solid solution at high pressures up to 55 GPa. *Physics and Chemistry of Minerals*, 41: 633–638.
- Vennari, C.E., and Williams, Q., 2018. A novel carbon bonding environment in deep mantle high-pressure dolomite. *American Mineralogist*, 103: 171–174.
- Walker, J., Hays, P., and Kasting, J., 1981. A negative feedback mechanism for the long-term stabilization of Earth's surface temperature. *Journal of Geophysical Research*, 86: 9776–9782.
- Walter, M.J., Kohn, S.C., Araujo, D., Bulanova, G.P., Smith, C.B., Gaillou, E., Wang, J., Steele, A., and Shirey, S.B., 2011. Deep mantle cycling of oceanic crust: Evidence from diamonds and their mineral inclusions. *Science*, 334: 54–57.
- Wang, F., Zhao, C., Xu, L., and Liu, J., 2022. Effects of hydrostaticity and Mn-substitution on dolomite stability at high pressures. *American Mineralogist*, 107: 2234–2241.
- Wang, X.J., Chen, L.H., Hofmann, A.W., Hanyu, T., Kawabata, H., Zhong, Y., Xie, L.W., Shi, J.H., Miyazaki, T., Hirahara, Y., Takahashi, T., Senda, R., Chang, Q., Vaglarov, B.S., and Kimura, J.I., 2018. Recycled ancient ghost carbonate in the Pitcairn mantle plume. *Proceedings of the National Academy of Sciences of the United States of America*, 115: 8682–8687.
- Yang, H., Lin, J.F., Hu, M.Y., Roskosz, M., Bi, W., Zhao, J., Alp, E.E., Liu, J., Liu, J., Wentzowitch, R.M., Okuchi, T., and Dauphas, N., 2019. Iron isotopic fractionation in mineral phases from Earth's lower mantle: did terrestrial magma ocean crystallization fractionate iron isotopes? *Earth and Planetary Science Letters*, 506: 113–122.
- Zhang, J., Martinez, I., Guyot, F., and Reeder, R.J., 1998. Effects of Mg-Fe²⁺ substitution in calcite-structure carbonates: Thermoelastic properties. *American Mineralogist*, 83: 280–287.
- Zhang, X.Y., Chen, L.H., Wang, X.J., Hanyu, T., Hofmann, A.W., Komiya, T., Nakamura, K., Kato, Y., Zeng, G., Gou, W.X., and Li, W.Q., 2022. Zinc isotopic evidence for recycled carbonate in the deep mantle. *Nature Communications*, 13: 6085.
- Zhao, C., Lü, C., Xu, L., Liang, L., and Liu, J., 2021. Raman signatures of the distortion and stability of MgCO₃ to 75 GPa. *American Mineralogist*, 106: 367–373.
- Zhao, C., Xu, L., Gui, W., and Liu, J., 2020. Phase stability and vibrational properties of iron-bearing carbonates at high pressure. *Minerals*, 10: 1142.

About the first author



HU Jun, male, born in 1997 in Yancheng, China; graduate student in materials science and engineering at Yanshan University, Qinhuangdao. He is currently interested in the high pressure-temperature synthesis and characterization of carbonate minerals. E-mail: hujun@stumail.yzu.edu.cn.

About the corresponding authors



YUE Donghui, male, born in 1991 in Heilongjiang, China. Ph.D. in physics; lecturer at the Mudanjiang Normal University, Heilongjiang. He has been focused on the physical properties and techniques for thermal transport under extreme conditions since 2014. E-mail: 15104409336@163.com.



LIU Jin, male, born in 1984 in Jiangsu, China. Ph.D. in mineral physics; staff scientist at the Center for High Pressure Science and Technology Advanced Research (HPSTAR), Beijing. He has been focused on the physics and chemistry of planetary materials under extreme conditions since 2007. E-mail: jinliuyc@foxmail.com.